Modified smoothed particle method and its application to transient heat conduction

EINDHOVEN UNIVERSITY OF TECHNOLOGY
Department of Mathematics and Computer Science

CASA-Report 12-13
May 2012

Modified smoothed particle method and its application to transient heat conduction

by

Q. Hou, Y. Fan

Centre for Analysis, Scientific computing and Applications
Department of Mathematics and Computer Science
Eindhoven University of Technology
P.O. Box 513
5600 MB Eindhoven, The Netherlands
ISSN: 0926-4507

Modified smoothed particle method and its application to transient heat conduction

Q. Hou, Y. Fan

Department of Mathematics and Computer Science, Eindhoven University of Technology, 5600 MB Eindhoven, The Netherlands

Abstract

Inspired by the idea of applying kernel approximation to Taylor series expansions proposed in the corrective smoothed particle method (CSPM), a modification is developed to improve the accuracy of the approximations especially for particles in the boundary region. The large global error of the function approximation in CSPM is reduced in the present method. The large local truncation error in the boundary region for the first derivative approximation and large local truncation error in the entire domain for the second derivative approximation are also resolved. The efficiency of the proposed method is demonstrated by solving one- and two-dimensional transient heat conduction problems.

Keywords: modified smoothed particle method, kernel approximation, Taylor series expansion, transient heat conduction

1. Introduction

As a meshfree, Lagrangian, particle method for solving fluid flow problems, the smoothed particle hydrodynamics (SPH) method was originally developed by Lucy [13], Gingold and Monaghan [8] independently in 1977 for the simulation of three-dimensional astrophysical problems. For details on the general aspects of SPH and its applications to astrophysical and cosmological flows, see the review papers [14, 15]. After its invention, SPH has been studied extensively and becomes a powerful tool for applications in numerous other areas; see the recent overview [12] and references therein. Libersky and Petschek [9] extended SPH to study the response of elastic bodies where material strength plays an important role, and surveyed the advantages and progress in this field [17]. Many other references can also be found in the review papers [1, 18].

Although SPH has been applied successfully in a broad spectrum of engineering problems, it has several inherent drawbacks, among which boundary deficiency [2] and tensile instability [5], are notable ones that can lead to low accuracy of the SPH approximations. Attempts to address these shortcomings led to the development of a number of variants of the original SPH method [1, 10, 12]. By combining the kernel approximation concept in SPH with a Taylor series expansion, a so-called corrective smoothed particle method (CSPM) has been developed by Chen *et al*. [4]. As an improvement to the standard SPH method, the CSPM algorithm not only remedies the boundary deficiency problem in SPH [4], but also avoids the tensile instability problem in stress wave propagation [5]. It has been applied to many dynamic problems such as heat conduction [4], elastodynamics [5, 6, 16], Burgers' equation [3] and elastoplastic dynamics [7]. However, the low accuracy in the approximations of the function and its second-order derivatives restricts its further development. Inspired by the idea of Chen [4], a modification to CSPM, which retains all high order derivative terms in the approximations of low order derivatives, is proposed herein to further improve the low accuracy in the approximations especially at the boundary region.

The paper is organized as follows. Section 2 gives a brief introduction to the conventional SPH method. The modified smoothed particle method is presented in Section 3, where local truncation error and global error are analyzed. Furthermore, a detailed comparison with CSPM is also presented. The applications of MSPM to several transient heat conduction problems are presented in Sections 4. Section 5 gives the conclusions.

2. Smoothed particle hydrodynamics

In the original SPH method, the kernel approximation of a function $f(\mathbf{x})$, $\mathbf{x} \in \mathbb{R}^3$ is given by

$$\langle f(\mathbf{x}) \rangle := \int_\Omega f(\boldsymbol{\xi}) W(\mathbf{x} - \boldsymbol{\xi}, h) d\boldsymbol{\xi}, \tag{2.1}$$

where $\langle \cdot \rangle$ denotes the approximation, $\mathbf{x}$ and $\boldsymbol{\xi}$ are position vectors. The weighting function $W(\mathbf{x} - \boldsymbol{\xi}, h)$ is generally called kernel, and the smoothing length h is a size measure of the support Ω of the kernel. The support is required to be compact, i.e. $W(\mathbf{x} - \mathbf{x}_j, h) = 0$, if $|\mathbf{x} - \mathbf{x}_j| \geqslant \kappa h$, where κ is a scale parameter, usually taken as 2. Using this property, spatial derivatives are transformed into their SPH approximations via integration by parts,

$$\begin{aligned} \langle \nabla f(\mathbf{x}) \rangle &= \int_\Omega \nabla f(\boldsymbol{\xi}) W(\mathbf{x} - \boldsymbol{\xi}, h) d\boldsymbol{\xi} \\ &= \int_S f(\boldsymbol{\xi}) W(\mathbf{x} - \boldsymbol{\xi}, h) \vec{n} dS - \int_\Omega f(\boldsymbol{\xi}) \nabla_{\boldsymbol{\xi}} W(\mathbf{x} - \boldsymbol{\xi}, h) d\boldsymbol{\xi} \\ &= \int_\Omega f(\boldsymbol{\xi}) \nabla_{\mathbf{x}} W(\mathbf{x} - \boldsymbol{\xi}, h) d\boldsymbol{\xi} \\ &= \nabla \langle f(\mathbf{x}) \rangle, \end{aligned} \tag{2.2}$$

where ∇ is the gradient operator and $\vec{n}$ is the outer unit normal on the surface S.

Another important concept in SPH is the so-called particle approximation. Provided domain Ω is divided into N parts (particles located at $\mathbf{x}_j$) with volumes ΔV_j ($j = 1, 2, \ldots, N$), the integrals in (2.1) and (2.2) are then approximated by the Riemann sums

$$\langle f(\mathbf{x}) \rangle \doteq \sum_j f(\mathbf{x}_j) W(\mathbf{x} - \mathbf{x}_j, h) \Delta V_j, \tag{2.3}$$

and

$$\langle \nabla f(\mathbf{x}) \rangle \doteq \sum_j f(\mathbf{x}_j) \nabla W(\mathbf{x} - \mathbf{x}_j, h) \Delta V_j. \tag{2.4}$$

The first-order derivative approximations in other forms can be found in [14].

In SPH the kernel $W(\mathbf{x} - \mathbf{x}', h)$ can be chosen differently based on the specific problem. It is generally required to have the following properties:

(i) normalization condition: $\sum_j W(\mathbf{x} - \mathbf{x}_j, h) \Delta V_j = 1$;

(ii) symmetry: $W(\mathbf{x} - \mathbf{x}_j, h) = W(\mathbf{x}_j - \mathbf{x}, h)$;

(iii) positivity: $W(\mathbf{x} - \mathbf{x}_j, h) \geqslant 0$;

(iv) δ-function consistency: $\lim_{h\to 0} W(\mathbf{x}-\mathbf{x}_j, h) = \delta(\mathbf{x}-\mathbf{x}_j)$, where δ is the Dirac delta function;

(v) monotonically decreasing with respect to $r := |\mathbf{x}-\mathbf{x}_j|$.

In SPH, the volume ΔV_j is further determined by mass/density ratio, i.e. $\Delta V_j = m_j/\rho_j$. In the following sections, the approximation symbol $\langle\cdot\rangle$ will be neglected, and the abbreviations $W := W(\mathbf{x}-\boldsymbol{\xi}, h)$ and $W_j := W(\mathbf{x}-\mathbf{x}_j, h)$ will be used, for simplicity. In addition, the accuracy of (2.3) and (2.4) depends upon the chosen kernel and smoothing length.

Remark 1 In particle methods, constant mass of each particle is assumed to ensure mass conservation. Consequently, it is only necessary for the volume ΔV_j to be further determined by $\Delta V_j = m_j/\rho_j$ when the density ρ_j is changing.

3. Modified smoothed particle method

Inspired by the idea of applying kernel approximation to a Taylor series expansion developed by Chen *et al.* [4], we propose a modified smoothed particle method (MSPM) in this section. To demonstrate the improvements, a comparison between the present method and the CSPM algorithm is described. The method will be introduced by a three-dimensional example. Its application to one- and two-dimensional problems can be easily implemented. The notations $\mathbf{x} = (x_1, x_2, x_3)$, $\boldsymbol{\xi} = (\xi_1, \xi_2, \xi_3)$ and $\mathbf{x}_j = (x_{j,1}, x_{j,2}, x_{j,3})$ are used.

The Taylor series of a function $f(\mathbf{x})$ is

$$f(\boldsymbol{\xi}) = f(\mathbf{x}) + \sum_{\alpha} \frac{\partial f}{\partial x_\alpha}\Big(\xi_\alpha - x_\alpha\Big) + \sum_{\alpha,\beta} \frac{1}{2!}\frac{\partial^2 f}{\partial x_\alpha \partial x_\beta}\Big(\xi_\alpha - x_\alpha\Big)\Big(\xi_\beta - x_\beta\Big) + \cdots, \tag{3.1}$$

where the indices $\alpha = 1, 2, 3$ and $\beta = 1, 2, 3$. By introducing two vectors $\mathbf{p}$ and $\mathbf{u}$:

$$\begin{aligned}\mathbf{p} = \Big(&\xi_1 - x_1, \xi_2 - x_2, \xi_3 - x_3, (\xi_1 - x_1)^2/2, (\xi_2 - x_2)^2/2, (\xi_3 - x_3)^2/2,\\ &(\xi_1 - x_1)(\xi_2 - x_2), (\xi_2 - x_2)(\xi_3 - x_3), (\xi_1 - x_1)(\xi_3 - x_3)\Big)\end{aligned} \tag{3.2}$$

and

$$\mathbf{u} = \left(\frac{\partial f}{\partial x_1}, \frac{\partial f}{\partial x_2}, \frac{\partial f}{\partial x_3}, \frac{\partial^2 f}{\partial x_1^2}, \frac{\partial^2 f}{\partial x_2^2}, \frac{\partial^2 f}{\partial x_3^2}, \frac{\partial^2 f}{\partial x_1 \partial x_2}, \frac{\partial^2 f}{\partial x_2 \partial x_3}, \frac{\partial^2 f}{\partial x_1 \partial x_3}\right)^{\mathrm{T}}, \tag{3.3}$$

the formulation (3.1) is rewritten as

$$f(\boldsymbol{\xi}) - f(\mathbf{x}) \doteq \mathbf{p}\,\mathbf{u}. \tag{3.4}$$

where third and higher order derivative terms have been neglected.

3.1. Kernel approximation of the derivatives

Multiplying both sides of (3.4) with the first derivative of the kernel $W_{\xi_\alpha} := \frac{\partial W(\mathbf{x}-\boldsymbol{\xi}, h)}{\partial \xi_\alpha}$ and integrating over Ω yields

$$\int_\Omega \Big(f(\boldsymbol{\xi}) - f(\mathbf{x})\Big) W_{\xi_\alpha} d\boldsymbol{\xi} = \int_\Omega \mathbf{p}\,\mathbf{u} W_{\xi_\alpha} d\boldsymbol{\xi}. \tag{3.5}$$

Similarly, with $W_{\xi_\alpha\xi_\beta} := \frac{\partial W(\mathbf{x}-\boldsymbol{\xi}, h)}{\partial \xi_\alpha \partial \xi_\beta}$, we obtain

$$\int_\Omega \Big(f(\boldsymbol{\xi}) - f(\mathbf{x})\Big) W_{\xi_\alpha\xi_\beta} d\boldsymbol{\xi} = \int_\Omega \mathbf{p}\,\mathbf{u} W_{\xi_\alpha\xi_\beta} d\boldsymbol{\xi}. \tag{3.6}$$

For simplicity we introduce another vector

$$\mathbf{w} := \Big(W_{\xi_1}, W_{\xi_2}, W_{\xi_3}, W_{\xi_1\xi_1}, W_{\xi_2\xi_2}, W_{\xi_3\xi_3}, W_{\xi_1\xi_2}, W_{\xi_2\xi_3}, W_{\xi_1\xi_3}\Big)^{\mathrm{T}}. \tag{3.7}$$

After writing the integrals in (3.5) and (3.6) into Riemann sums, a linear system consisting of nine equations is obtained

$$\mathbf{Au} = \mathbf{b}, \quad \text{or} \quad A_{IJ}u_J = b_I, \quad I, J = 1, 2, \ldots, 9, \tag{3.8}$$

where

$$A_{IJ} = \sum_j w_I(\mathbf{x}_j) p_J(\mathbf{x}_j) \Delta V_j, \tag{3.9}$$

and

$$b_I = \sum_j \Big(f(\mathbf{x}_j) - f(\mathbf{x})\Big) w_I(\mathbf{x}_j) \Delta V_j. \tag{3.10}$$

Vector $\mathbf{b}$ contains all information of the function f. When identical volume is used for all the particles, the term ΔV_j in both sides of (3.8) cancels out, under which sense the particles can be referred to as nodes or grid points but without connectivity.

Remark 2 Retaining third-order derivatives in the Taylor series expansion (3.1) would lead to a system containing 19 algebraic equations. With the increase of higher-order derivatives remaining in (3.1), the number of algebraic equations increases rapidly and more cost is needed to compute $\mathbf{u}$. This is the reason why only up to first-order derivative terms are retained in most of the meshfree methods.

3.2. Kernel approximation of the function

By multiplying both sides of (3.4) with W, integrating over Ω and writing the integral in Riemann summation form, we obtain

$$\sum_j \Big(f(\mathbf{x}_j) - f(\mathbf{x})\Big) W_j \Delta V_j = \sum_j \mathbf{p}\,\mathbf{u} W_j \Delta V_j. \tag{3.11}$$

Then the reconstructed function is obtained as

$$f(\mathbf{x}) = \frac{1}{\sum_j W_j \Delta V_j} \Bigg(\sum_j f(\mathbf{x}_j) W_j \Delta V_j - \sum_j \mathbf{p}\,\mathbf{u} W_j \Delta V_j \Bigg). \tag{3.12}$$

Substitution of all the derivatives u_J, $(J = 1, \cdots, 9)$ obtained from (3.8) into (3.12) gives the estimated function values.

Remark 3 For time dependent PDEs, kernel estimate of the function (3.12) is rarely performed, because function values at previous time step are used to get the approximated derivatives from (3.8). If the function itself appears in the PDEs, function values are also taken from the previous time step.

3.3. Comparing with CSPM

Neglecting all the derivative terms in (3.12), function approximation in MSPM is reduced to that in CSPM

$$f(\mathbf{x}) := \frac{\sum_j f(\mathbf{x}_j) W_j \Delta V_j}{\sum_j W_j \Delta V_j}. \tag{3.13}$$

For interior particles, the supports of the corresponding kernels have no overlap with the boundaries of the domain, formula (3.13) is further reduced to the conventional SPH kernel approximation (2.3) due to the normalization condition $\sum_j W_j \Delta V_j = 1$. Owing to the symmetry of the kernel function, we have $\sum_j (\mathbf{x}_j - \mathbf{x}) W_j \Delta V_j = \mathbf{0}$. Therefore, the truncation errors in (3.13) and (2.3) are second order. However, for particles near or at the boundaries, $\sum_j W_j \Delta V_j \neq 1$ because the support of W_j is truncated by the boundary. Consequently, the truncation error in (3.13) degenerates to first order, and the function approximation (2.3) even does not have zero-order accuracy [6].

By retaining up to first-order derivative terms in (3.5) and up to second-order derivative terms in (3.6), we obtain kernel approximations of the derivatives in CSPM

$$\widetilde{\mathbf{A}}\mathbf{u} = \mathbf{b}, \tag{3.14}$$

where $\widetilde{\mathbf{A}}$ is the same as $\mathbf{A}$ defined in (3.8) except that $A_{IJ} = 0$ ($I = 1, 2, 3,\ J = 4, 5, \ldots, 9$), $\mathbf{u}$ is the same as defined in (3.3) and $\mathbf{b}$ is defined in (3.10).

The kernel function plays an essential role in meshfree methods. The computationally efficient and widely used cubic spline function is chosen as the kernel in this article,

$$W_j := \frac{G}{h^\lambda} \begin{cases} 1 - 1.5q^2 + 0.75q^3, & 0 \leqslant q < 1; \\ 0.25(2-q)^3, & 1 \leqslant q < 2; \\ 0, & q \geqslant 2; \end{cases} \tag{3.15}$$

where $q := |\mathbf{x}_j - \mathbf{x}|/h$, λ indicates the dimension of the problem, and the normalized coefficient G equals to $2/3$, $10/(7\pi)$ and $1/\pi$ for $\lambda = 1, 2, 3$, respectively. The first and second derivatives of the kernel function, $w_I(\mathbf{x}_j)$ in (3.9), are determined by

$$\frac{\partial W(\mathbf{x}_j)}{\partial x_\alpha} := \frac{1}{h}\frac{dW}{dq}\frac{x_\alpha - x_{j,\alpha}}{r} \tag{3.16}$$

$$\frac{\partial^2 W(\mathbf{x}_j)}{\partial x_\alpha \partial x_\beta} := \frac{1}{h^2}\frac{d^2 W}{dq^2}\frac{(x_\alpha - x_{j,\alpha})(x_\beta - x_{j,\beta})}{r^2} + \frac{1}{h}\frac{dW}{dq}\left(\frac{\delta_{\alpha\beta}}{r} - \frac{(x_\alpha - x_{j,\alpha})(x_\beta - x_{j,\beta})}{r^3}\right) \tag{3.17}$$

where $\delta_{\alpha\beta}$ is the Kronecker delta, and $\alpha, \beta = 1, 2, 3$.

3.4. Weight functions: partition of nullity

To describe the weight functions, a one-dimensional problem is investigated for simplicity. The approximated derivatives solved from (3.8) are

$$\begin{pmatrix} f'(x) \\ f''(x) \end{pmatrix} = \mathbf{A}^{-1} \sum_j \mathbf{F}_j f_j, \tag{3.18}$$

where

$$\mathbf{A} = \begin{pmatrix} \sum_j (x_j - x) W_{j,x} \Delta V_j & \sum_j (x_j - x)^2 / 2 W_{j,x} \Delta V_j \\ \sum_j (x_j - x) W_{j,xx} \Delta V_j & \sum_j (x_j - x)^2 / 2 W_{j,xx} \Delta V_j \end{pmatrix}, \tag{3.19}$$

$$\mathbf{F}_j = \begin{pmatrix} W_{j,x}\Delta V_j - \delta_{ij} \sum_j W_{j,x} \Delta V_j \\ W_{j,xx}\Delta V_j - \delta_{ij} \sum_j W_{j,xx} \Delta V_j \end{pmatrix}, \tag{3.20}$$

with $f_j := f(x_j)$, $W_{j,x} := W_x(x - x_j, h)$ and $W_{j,xx} := W_{xx}(x - x_j, h)$.

We rewrite equation (3.18) as

$$f^{(k)} = \sum_j \Phi_j(k) f_j, \quad k = 1, 2, \tag{3.21}$$

where $f^{(k)}$ equals the kth derivative of $f(x)$, and

$$\begin{aligned} \Phi_j(1) &= (1, 0)\mathbf{A}^{-1}\mathbf{F}_j, \\ \Phi_j(2) &= (0, 1)\mathbf{A}^{-1}\mathbf{F}_j. \end{aligned} \tag{3.22}$$

The function $\Phi_j(k)$ depends on the employed kernel and can be viewed as weight functions in FDM or shape functions in FEM. We call them weight functions herein because they are used to solve the PDEs in strong form and generate the weight coefficients for the derivatives. The weight functions form a partition of nullity (PN), i.e. $\sum_j \Phi_j(k) = 0$, $(k = 1, 2)$. This property is important for numerical accuracy and can be proved as follows:

$$\sum_j \Phi_j(1) = (1, 0)\mathbf{A}^{-1} \sum_j \mathbf{F}_j = (1, 0)\mathbf{A}^{-1}(0, 0)^{\mathrm{T}} = 0,$$

and similarly $\sum_j \Phi_j(2) = 0$.

Although the property is demonstrated for one-dimensional derivatives, it holds for multi-dimensional problems too. The weight function in standard SPH derivatives (2.4) does not have the property. Substituting the solved derivatives into (3.12), the approximated function and the corresponding weight function for function approximation can be obtained. These weight functions (shape functions) can be used to solve PDEs in weak form, but special attention is needed for the enforcement of the essential boundary conditions [10].

3.5. Error estimate

For easy explanation, the local truncation error in the proposed method is presented by considering a one-dimensional system. Accordingly, (3.1) is reduced to

$$f(\xi) = f(x) + f'(x)(\xi - x) + \frac{1}{2} f''(x)(\xi - x)^2 + O((\xi - x)^3). \tag{3.23}$$

By multiplying both sides with W_ξ, integrating over the domain Ω, and then subtracting (3.5), we obtain

$$(f'(x) - \langle f'(x) \rangle) \int_\Omega (\xi - x) W_\xi d\xi = -(f''(x) - \langle f''(x) \rangle) \int_\Omega \frac{1}{2}(\xi - x)^2 W_\xi d\xi + O(h^3). \tag{3.24}$$

With respect to the cubic spline kernel, its first derivative W_ξ is antisymmetric, and satisfies the normalization condition $\int_\Omega (\xi - x) W_\xi d\xi = 1$ (see [11] for details). Owing to the antisymmetry property, the integral of $(\xi - x)^2 W_\xi$ vanishes for points far from the system boundary. Together with the normalization condition, the local truncation error of the first derivative approximation is

$$\tau_1 := f'(x) - \langle f'(x) \rangle = O(h^3). \tag{3.25}$$

For points near or on the boundaries, truncation of the kernel by the boundary results in $\int_\Omega (\xi - x) W_\xi d\xi \neq 1$ and $\int_\Omega \frac{1}{2}(\xi - x)^2 W_\xi d\xi \neq 0$. If we assume $\int_\Omega (\xi - x) W_\xi d\xi \geq C$, the local error becomes $\tau_1 = O(h^2)$, because $|f''(x) - \langle f''(x) \rangle|$ is bounded and $\int_\Omega \frac{1}{2}(\xi - x)^2 W_\xi d\xi \leq Ch^2$, here C is a generic positive constant.

Similarly, we have

$$\begin{aligned}
&(f'(x) - \langle f'(x)\rangle) \int_\Omega (\xi - x) W_{\xi\xi} d\xi \\
=& -(f''(x) - \langle f''(x)\rangle) \int_\Omega \frac{1}{2}(\xi - x)^2 W_{\xi\xi} d\xi \\
&+ f'''(x) \int_\Omega \frac{1}{6}(\xi - x)^3 W_{\xi\xi} d\xi + O(h^4).
\end{aligned} \tag{3.26}$$

For the cubic spline kernel, its second derivative $W_{\xi\xi}$ is symmetric, and satisfies the normalization condition $\int_\Omega (\xi - x) W_{\xi\xi}/2 d\xi = 1$ (see [11]). Consequently, for interior points, the local truncation error of the second derivative approximation is

$$\tau_2 := f''(x) - \langle f''(x)\rangle = O(h^4). \tag{3.27}$$

For points near or on the boundaries, truncation of the kernel leads to $\int_\Omega \frac{1}{2}(\xi - x)^2 W_\xi d\xi \neq 1$ and $\int_\Omega (\xi - x) W_{\xi\xi} d\xi \neq 0$. If we assume $\int_\Omega \frac{1}{2}(\xi - x)^2 W_\xi d\xi \geq C$, and then the local error becomes $\tau_2 = O(h)$, because $|f'(x) - \langle f'(x)\rangle|$ is bounded and $\int_\Omega (\xi - x) W_\xi d\xi \leq Ch$.

Similarly, the local error of the function approximation $\tau_0 := f(x) - \langle f(x)\rangle$ is $O(h^4)$ for interior points, and $O(h^3)$ for points near the boundary. As mentioned before, function approximation can be used in the weak form of PDEs, but it is rarely used for equations in strong form. Therefore, the approximation of $f(x)$, $f'(x)$ and $f''(x)$ has accuracy of h^3, h^2 and h, respectively.

Remark 4 In above assumptions $\int_\Omega (\xi - x) W_\xi d\xi \geq C$ and $\int_\Omega \frac{1}{2}(\xi - x)^2 W_\xi d\xi \geq C$, constant C depends on the shape of the domain. These assumptions are reasonable because most of the considered domains are regular.

4. Numerical examples

In this section, we will illustrate our method with two typical initial boundary heat conduction problems. The spacial derivatives are approximated using the present method, while the temporal derivative is integrated by the forward Euler's method, which is conditionally stable. The critical time step size is related to the particle spacing and smoothing length. To meet the stability condition, the critical time step that is $(\Delta x)^2/2^\lambda$ over all particles was found in [4], where Δx is the particle distance.

4.1. 1D heat conduction

Consider the following problem

$$\frac{\partial T}{\partial t} = \frac{\partial^2 T}{\partial x^2}, \quad 0 < x < \pi, \ \ t > 0 \tag{4.1}$$

with homogeneous Dirichlet boundary condition

$$T|_{\partial\Omega} = 0, \tag{4.2}$$

and initial condition

$$T(x, 0) = 10 \sin x, \quad 0 \leq x \leq \pi, \tag{4.3}$$

where the exact solution is

$$T(x, t) = 10 e^{-t} \sin x. \tag{4.4}$$

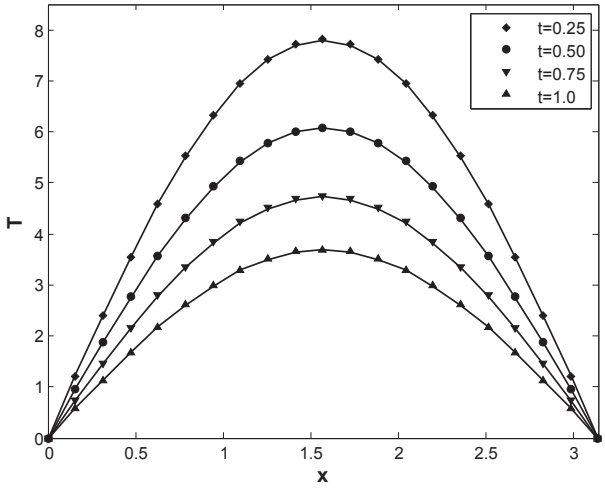

Fig. 1 Numerical results (symbols) and exact solution (solid lines) for T with $\Delta t = 0.001$ for t = 0.25, t = 0.5, t = 0.75 and t = 1.0, respectively.

In the simulation of the above heat equation, $N_p = 21$ particles, scale factor $C_h = 1.2$, and time-step size $\Delta t = 0.001$ are adopted. In Fig. 1, the exact solutions $T(x,t) = 10e^{-t}\sin x$ (solid lines) are plotted in comparison with the numerical results (symbols) when $t = 0.25$, $t = 0.5$, $t = 0.75$ and $t = 1$. It is evident that the MSPM results agree with the exact solutions very well.

The variations of the L^2 norm errors with different number of particles are shown in Table 1. For comparison the numerical error of CSPM is also presented. The numbers of particles are 21, 31, 41, 51 and 61. It is evident that the numerical behaviour of the present method is better than that of CSPM. This verifies the theoretical analysis given in Section 3.3. The numerical error is of the order $O(h^2)$. It is consistent with the theoretical results as demonstrated in Section 3.5, and is higher than the accuracy order in the second derivative approximation. This is because large pointwise errors happened in the boundary region are largely improved due to the enforcement of boundary conditions.

Table 1: Effect of the number of particles N_p on the L^2-norm errors: ^{a} CSPM, ^{b} MSPM.

Δx	Error^a	Error^b	Error$^b/(\Delta x)^2$
$\pi/20$	0.0590	0.0566	2.30
$\pi/30$	0.0302	0.0293	2.67
$\pi/40$	0.0167	0.0162	2.63
$\pi/50$	0.0089	0.0086	2.19

4.2. 2D heat conduction

Considering the following heat conduction problem in a 2-D plate

$$\frac{\partial T}{\partial t} = \frac{\partial^2 T}{\partial^2 x} + \frac{\partial^2 T}{\partial^2 y}, \quad 0 < x, y < \pi, \quad t > 0 \tag{4.5}$$

with boundary condition

$$T|_{\partial\Omega} = 0 \tag{4.6}$$

and initial condition

$$T(x, y, 0) = \sin x \sin y, \quad 0 \le x, y \le \pi, \tag{4.7}$$

where the exact solution is

$$T(x, y, t) = e^{-2t} c \sin x \sin y. \tag{4.8}$$

The distribution of $N_p = 21 \times 21$ particles with equal spacing $\Delta x = \Delta y$ is employed in MSPM. The smoothing length h is taken as $1.2\Delta x$. The time step size is $\Delta t = 10^{-4}$. The numerical results at time $t = 0.2$ s are depicted in Fig. 2, where the exact solutions are also plotted in comparison with the numerical results. The MSPM solution agrees with the exact solutions so well that the difference between them is hardly visible. Figure 3 gives the time variance of temperature at the centre of the plate. As expected, the MSPM calculations are in good correlation with the exact solution, and the small discrepancy due to the coarse model can be eliminated by employing more particles.

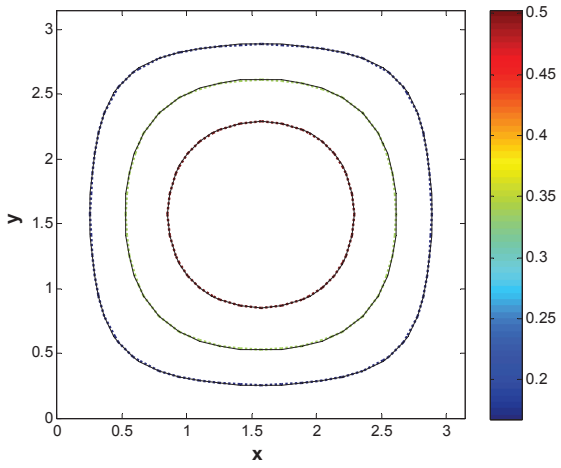

Fig. 2 Temperature distribution in the plate at time $t = 0.2$ s computed by MSPM with 21×21 particles (dotted lines), with comparison with the exact solution (solid lines).

The L^2 norm errors with different number of particles are shown in Table 2. As expected the numerical error is of the order $O(h)$, which is consistent with the theoretical analysis in Section 3.5. The relationship

Table 2: Effect of the number of particles N_p on the L^2-norm error.

Δx	Error	Error/Δx
$\pi/10$	0.0678	0.22
$\pi/20$	0.0359	0.23
$\pi/30$	0.0255	0.24
$\pi/40$	0.0204	0.26

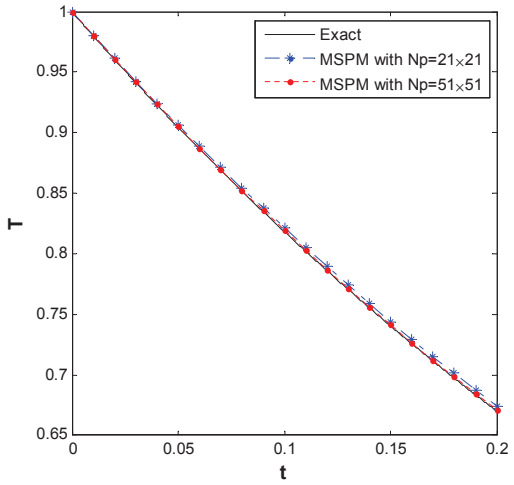

Fig. 3 Time history of the temperature at the centre of the plate computed by MSPM with different number of particles.

of the error and the scale factor as shown in Fig. 4 indicates that the error decreases with the decrease of the smoothing length with small variations.

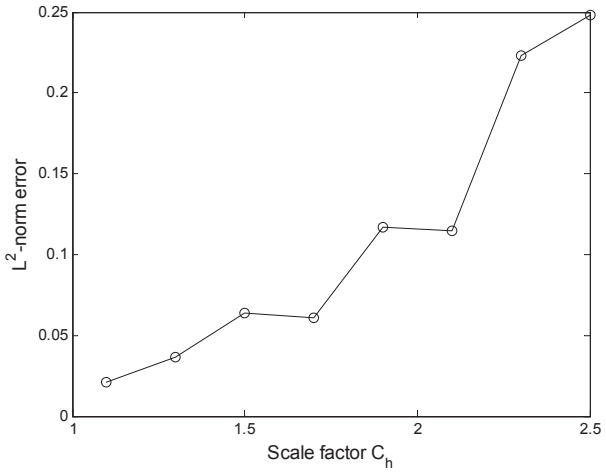

Fig. 4 Effect of the scale factor C_h on the L^2-norm error with $N_p = 21 \times 21$ particles.

5. Conclusions

Based on the technique of combining kernel approximation and Taylor series expansions as proposed in the corrective smoothed particle method (CSPM) by Chen *et al.* [4], a new meshfree method, the modified smoothed particle method (MSPM), is developed and successfully applied to initial boundary value problems in heat conduction. The performance of the method are demonstrated by two heat conduction

problems.

Acknowledgments

The authors would like to thank Prof. R.M.M. Mattheij and Dr. A.S. Tijsseling for their valuable comments. The first author is grateful to the China Scholarship Council (CSC) for financially supporting his PhD studies.

References

[1] T. Belytschko, Y. Krongauz, D. Organ, M. Flemming and P. Krysl (1996). Meshless methods: an overview and recent developments. Comput. Meth. Appl. Mech. Eng. 139: 3–47.

[2] T. Belytschko, T. Krongaus, J. Dolbow and C. Gerlach (1998). On the completeness of meshfree particle methods. Int. J. Numer. Methods Eng. 43: 785–819.

[3] J.K. Chen and J.E. Beraun (2000). A generalized smoothed particle hydrodynamics method for nonlinear dynamic problems. Comput. Meth. Appl. Mech. Eng. 190: 225–239.

[4] J.K. Chen, J.E. Beraun and T.C. Carney (1999). A corrective smoothed particle method for boundary value problems in heat conduction. Int. J. Numer. Methods Eng. 46: 231–252.

[5] J.K. Chen, J.E. Beraun and C.J. Jih (1999). An improvement for tensile instability in smoothed particle hydrodynamics. Comput. Mech. 23: 279–287.

[6] J.K. Chen, J.E. Beraun and C.J. Jih (1999). Completeness of corrective smoothed particle method for linear elastodynamics. Comput. Mech. 24: 273–285.

[7] J.K. Chen, J.E. Beraun and C.J. Jih (2001). A corrective smoothed particle method for transient elastoplastic dynamics. Comput. Mech. 27: 177–187.

[8] R.A. Gingold and J.J. Monaghan (1977). Smoothed particle hydrodynamics: theory and application to non-spherical stars. Mon. Not. R. Astron. Soc. 181: 375–389.

[9] L.D. Libersky, A.G. Petschek, T.C. Carney, J.R. Hipp and F.A. Allahdadi (1993). High strain Lagrangian hydrodynamics: A threedimensional SPH code for dynamic material response. J. Comput. Phys. 109: 67–75.

[10] S.F. Li and W.K. Liu (2002). Meshfree and particle methods and their applications. Appl. Mech. Rev. 55(1): 1–34.

[11] G.R. Liu and M.B. Liu (2003). Smoothed Particle Hydrodynamics: A Meshfree Particle Method. World Scientific, Singapore.

[12] M.B. Liu and G.R. Liu (2010). Smoothed particle hydrodynamics (SPH): An overview and recent developments. Arch. Comput. Meth. Eng. 17: 25–76.

[13] L.B. Lucy (1977). A numerical approach to the testing of fission process. Astron. J. 88: 1013–1024.

[14] J.J. Monaghan (1992). Smoothed particle hydrodynamics. Annu. Rev. Astron. Astrophys. 1992. 30: 543–574.

[15] J.J. Monaghan (2005). Smoothed particle hydrodynamics. Rep. Prog. Phys. 68: 1703–1759.

[16] H. Ostad and S. Mohammadi (2008). A field smoothing stabilization of particle methods in elastodynamics. Finite Elem. Anal. Des. 44: 564–579.

[17] P.W. Randles and L.D. Libersky (1996). Smoothed particle hydrodynamics: Some recent improvements and applications. Comput. Meth. Appl. Mech. Eng. 138: 375–408.

[18] R. Vignjevic (2004). Review of development of the smooth particle hydrodynamics. Dynamics and Control of Systems and Structures in Space (DCSSS), 6th Conference, Riomaggiore, Italy, July 2004.

PREVIOUS PUBLICATIONS IN THIS SERIES:

Number	Author(s)	Title	Month
12-09	C.R. Prins J.H.M. ten Thije Boonkkamp T.W. Tukker W.L. IJzerman	An inverse method for the design of TIR collimators to achieve a uniform color light beam	Apr. '12
12-10	W. Hundsdorfer A. Mozartova V. Savcenco	Monotonicity conditions for multirate and partitioned explicit Runge-Kutta schemes	May '12
12-11	J. Bogers K. Kumar P.H.L. Notten J.F.M. Oudenhoven I.S. Pop	A multiscale domain decomposition approach for chemical vapor deposition	May '12
12-12	K. Kumar T.L. van Noorden I.S. Pop	Upscaling of reactive flows in domains with moving oscillating boundaries	May '12
12-13	Q. Hou Y. Fan	Modified smoothed particle method and its application to transient heat conduction	May '12

Ontwerp: de Tantes,
Tobias Baanders, CWI